Joint Distributed Beamforming and Backscatter Cooperation for UAV-Assisted WPSNs

Zhi Mao*, Fengye Hu*, Qihao Li†, Wen Wu†, and Xuemin (Sherman) Shen†
*College of Communication Engineering, Jilin University
†Department of Electrical and Computer Engineering, University of Waterloo
Email: *zhimao17@mails.jlu.edu.cn, hufy@jlu.edu.cn, †{qihao.li, w77wu, sshen}@uwaterloo.ca

GLOBECOM 2021 - 2021 IEEE Global Communications Conference | 978-1-7281-8104-2/21/$31.00 ©2021 IEEE | DOI: 10.1109/GLOBECOM46510.2021.9685412

***Abstract*—Unmanned aerial vehicle (UAV)-assisted wireless powered sensor networks (WPSNs) have emerged as a promising paradigm for charging sensor nodes' batteries in remote areas. However, the sum-throughput of overall sensor nodes can dramatically decrease due to their long-distance transmission to the UAV. In this paper, we propose a joint distributed beamforming and backscatter cooperation (BC) scheme to enhance the sum-throughput of UAV-assisted WPSNs with various types of sensor nodes. In particular, we consider the BC mechanism which leverages other types sensor nodes with constructive multi-path signals to enhance the long-distance transmission of same-type sensor nodes. We maximize the sum-throughput by jointly optimizing the distributed backscattering, distributed beamforming and time allocation. The sum-throughput maximization problem is difficult to be solved directly due to the coupling among optimizing variables. We decompose the problem into a BC subproblem and a time allocation subproblem, and propose a two-step scheme to solve them. First, for the BC subproblem, we derive closed-form low-complexity distributed beamforming solutions and distributed backscattering solutions to maximize the signal-to-noise ratios of the same-type sensor nodes. Second, for the time allocation subproblem, we derive the closed-form solutions according to KKT conditions. Simulation results are provided to demonstrate that the proposed joint distributed beamforming and BC scheme can increase the sum-throughput as compared to conventional distributed beamforming schemes.**

I. Introduction

Wireless powered sensor networks (WPSNs) are envisioned as a promising paradigm for self-sustainable Internet of Things (IoTs) to reduce the frequency of manually battery replacement and charging. However, in the conventional wireless powered network, power transmitters are usually deployed at fixed locations, which cover limited areas and makes it difficult for far sensor nodes to achieve good power transfer efficiency over long-distance transmission [1], [2]. To overcome this issue, the unmanned aerial vehicle (UAV) introduced as an assisted component is employed as a mobile power transmitter and an information receiver in WPSNs [3]. Specifically, in the UAV-assisted WPSN, the UAV flies from one area to another to charge distributed sensor nodes through wireless power transfer (WPT) techniques. Then, the sensor nodes send the measurement information to the UAV by using the harvested energy [4]–[7]. Despite the assistance of the UAV, the long-distance transmission issue remains prominent during the WPT. That is because, to efficiently charge sensor nodes and collect the measurement information, the UAV has to move sufficiently close to sensor nodes. Thus, the UAV have to consume more time and energy to follow a predesigned trajectory to charge distributed sensor nodes.

The distributed beamforming technique has been used to address the long-distance transmission issue in the UAV-assisted WPSNs [8], [9]. After information sharing and synchronization, a group of sensor nodes can cooperate to form a virtual antenna array for transmitting common information to a UAV. In this way, the received signal at the UAV can be coherently combined to enlarge the signal-to-noise ratio (SNR) [8], [10]. As the UAV moves close to the ground, only a small number of same-type sensor nodes in the coverage of the UAV cooperate for distributed beamforming. As such, the distributed beamforming may be incapable of supporting the long-distance transmission due to a low SNR. To overcome this issue, we introduce backscatter-enabled relaying nodes integrated with passive components in the network, which can passively reflect the received signals from the sensor nodes to the UAV. In this way, the backscatter nodes are able to produce constructive multi-path signals to improve the received SNR [11], [12].

In this paper, we propose a joint distributed beamforming and backscatter cooperation (BC) scheme to enhance the sum-throughput of a UAV-assisted WPSN. Specifically, the UAV-assisted WPSN adopts a harvest-then-transmit (HTT) strategy for energy harvesting and information transmission between the UAV and the sensor nodes. In the energy harvesting phase, sensor nodes of different types simultaneously harvest energy transmitted from the UAV. Then, in the information transmission phase, sensor nodes of different types transmit information in a time division multiple access (TDMA) manner. A group of the same-type sensor nodes transmit their common information together through distributed beamforming. Meanwhile, all the sensor nodes of other types act as backscatter nodes to reflect signals from the transmitted sensor nodes to the UAV. Extensive simulation results validate the effectiveness of the proposed scheme in enhancing the sum-throughput performance. The main contributions of this paper are as follows.

- We propose a joint distributed beamforming and BC scheme for uplink transmission in the UAV-assisted WPSN. Specifically, the transmitted signals of a group of same-type sensor nodes are backscattered by the sensor nodes of other types to enhance the SNR at the UAV.
- We formulate a non-convex sum-throughput maximiza-

978-1-7281-8104-2/21/$31.00 ©2021 IEEE

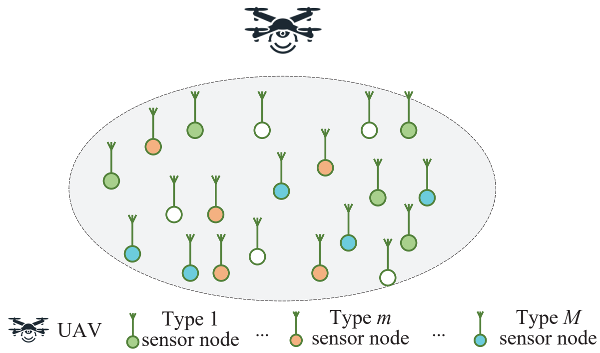

Fig. 1. The UAV-assisted WPSN with various types of single-antenna sensor nodes.

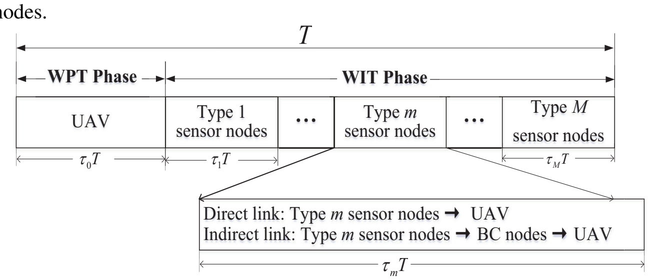

Fig. 2. The transmission protocol in the UAV-assisted WPSN.

tion problem by jointly optimizing the distributed backscattering, distributed beamforming, and time allocation. It is difficult to directly solve the sum-throughput maximization problem because of the coupling among optimizing variables. Thus, we decompose the problem into a BC subproblem and a time allocation subproblem.

- We propose a two-step scheme to solve these two subproblems. First, we derive the closed-form expressions of low-complexity distributed beamforming solutions and distributed backscattering solutions to solve the BC subproblem. Second, we derive the closed-form expressions of the solutions for the time allocation subproblem according to KKT conditions.

II. System Model

A. Considered Scenario

We consider a UAV-assisted WPSN which consists of one UAV and a large number of sensor nodes uniformly deployed in remote areas, as shown in Fig. 1. There are M types of sensor nodes and the number of type m sensor nodes is N_m (It is assumed $N_1 = \cdots = N_M = N$ for simplicity in derivation). We assume that both the sensor nodes and the UAV are equipped with only one antenna and operate over the same frequency band. The UAV is dispatched as an aerial energy transmitter to charge various sensor nodes on the ground. It is assumed that there is no initial energy in the batteries of sensor nodes which are equipped with a radio frequency (RF) harvester to collect RF energy. In addition, the harvested energy of each sensor node is used to transmit measurement information to the UAV via joint distributed beamforming and BC. When a group of same-type sensor nodes transmit their common information to the UAV, all the sensor nodes of other sensor types act as backscatters to provide BC. All the sensor nodes can enable the backscatter capability to reflect the received RF signals without energy consumption. Moreover, only the sensor nodes of the same type can share the common information which is obtained via information sharing or measuring the same information [13]–[15]. Since the UAV transfers the power and receives the signal through line-of-sight (LoS) links, only distance-dependent pathloss is considered in the model. Specifically, wireless channels are quasi-static flat-fading, i.e., channels keep constant in each block, but change independently from one block to another. Accordingly, given the distance D between the UAV and a sensor node, the channel power gain is given by $|h|^2 = 10^{-3}\rho^2 D^{-\alpha}$, where channel h is a complex random variable. ρ represents the channel shadowing which is assumed to follow the Rayleigh distribution [2], [16], α is the channel pathloss exponent.

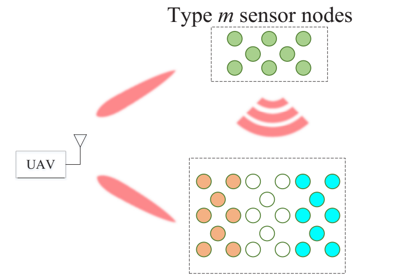

Fig. 3. The joint distributed beamforming and backscatter cooperation scheme in the UAV-assisted WPSN.

The UAV-assisted WPSN adopts the HTT protocol [2] for energy harvesting and information transmission between the UAV and sensor nodes, as shown in Fig. 2. In particular, each block with duration T is divided into two phases: WPT phase and wireless information transmission (WIT) phase. In the WPT phase whose duration is $\tau_0 T$, $0 < \tau_0 \leqslant 1$, all sensor nodes harvest wireless energy from the UAV simultaneously. The WIT phase has a duration of $(1-\tau_0)T$. This phase is divided into M portions for M sensor types and type m sensor nodes are assigned with duration $\tau_m T,\ 0 < m \leqslant M$.

Type m sensor nodes transmit their common information via the joint distributed beamforming and BC, as shown in Fig. 3. We assume that the information synchronization has been completed in type m sensor nodes before their information transmission [13], [14]. After WPT phase, all type m sensor nodes transmit their common information by using the harvested energy. The signals are transmitted in two types of links: direct link and indirect link. In the direct link, signals are transmitted from the type m sensor nodes to the UAV directly. In the indirect link, sensor nodes of all other $M-1$ sensor types provide distributed BC and reflect signals from type m sensor nodes to the UAV to improve the received SNR. The backscattering coefficient at a cooperative sensor node is adjusted by tuning the load impedance of antenna at itself.

To sum up, the signal transmission model based on the two-phase HTT protocol is given in following two subsections.

B. WPT Phase

During WPT phase, the UAV charges all sensor nodes simultaneously through WPT. Denote by S_{mn} the n^{th} sensor node of m^{th} sensor type, then the received signal at S_{mn} is given by $y_{mn}^{s}=\sqrt{P_a}h_{mn}x_a+z_{mn}$, where x_a and P_a are the normalized transmitted signal and the transmit power of the UAV, respectively. $h_{mn}\in\mathbb{C}^{1\times 1}$ is the channel from the UAV to S_{mn}. In addition, $z_{mn}\sim\mathcal{CN}(0,\sigma_{mn}^2)$ is the additive white Gaussian noise (AWGN) at the receiving antenna of S_{mn}. The received signal power at S_{mn} can be obtained by

$$P_{mn}^{Re}=\mathbb{E}\left[\left|y_{mn}^{s}\right|^2\right]=\left|\sqrt{P_a}h_{mn}\right|^2+\sigma_{mn}^2\approx P_a\left|h_{mn}\right|^2. \quad (1)$$

Since the output of a practical energy harvesting (EH) circuit is always finite, a nonlinear EH model in [17] with upper boundary M_{mn}^{EH} is adopted in this paper, i.e.,

$$P_{mn}^{EH}=\frac{\Psi_{mn}-M_{mn}^{EH}\Omega_{mn}}{1-\Omega_{mn}},\ \Omega_{mn}=\frac{1}{1+e^{a_{mn}b_{mn}}}, \quad (2)$$

$$\Psi_{mn}=\frac{M_{mn}^{EH}}{1+e^{-a_{mn}\left(P_{mn}^{Re}-b_{mn}\right)}}. \quad (3)$$

Here, P_{mn}^{EH} is the practical EH power at S_{mn} which is a conventional logistic function with respect to the received signal power P_{mn}^{Re} [17]. Here, a_{mn} and b_{mn} are parameters related to the detailed EH circuit. M_{mn}^{EH} is the maximum output of the EH circuit at S_{mn}. Thus, the energy harvested at S_{mn} in this phase can be obtained by $E_{mn}=P_{mn}^{EH}\tau_0 T$.

C. WIT Phase

The WIT phase is divided into M portions unequally for M sensor types, as shown in Fig. 2. Within $\tau_m T$ amount of time assigned to type m sensor nodes, the sensor nodes of sensor type m exhaust the harvested energy to transmit their common information to the UAV. The transmitted signal at S_{mn} can be expressed as:

$$x_{mn}=\sqrt{\frac{E_{mn}}{\tau_m T}}e^{j\theta_{mn}^{Tx}}s_m, \quad (4)$$

where θ_{mn}^{Tx} is the phase of transmitted signal at S_{mn}, and s_m is the baseband transmitted signal of common information of type m sensor nodes. When type m sensor nodes transmit their common information to the UAV, the rest sensor nodes act as distributed backscatters. Denote by $\boldsymbol{x}_m=\left[x_{m1},\cdots,x_{mn},\cdots,x_{mN}\right]^T$ the distributed beamforming vector at type m sensor nodes. Then, the received signal at the UAV can be expressed as

$$y_m^a=\left(\boldsymbol{g}_{d_m}^T+\boldsymbol{g}_{r_m}^T\boldsymbol{\Phi}_m\boldsymbol{H}_m\right)\boldsymbol{x}_m+z', \quad (5)$$

where $\boldsymbol{g}_{d_m}\in\mathbb{C}^{N\times 1}$ is the channel vector from the type m sensor nodes to the UAV. We assume that the channel reciprocity holds for the downlink and uplink and thus $\boldsymbol{g}_{d_m}=\left[h_{m1},\cdots,h_{mn},\cdots,h_{mN}\right]^T$. $\boldsymbol{g}_{r_m}\in\mathbb{C}^{N(M-1)\times 1}$ is the channel vector from the BC nodes to the UAV. $\boldsymbol{H}_m\in\mathbb{C}^{N(M-1)\times N}$ is the channel matrix from the type m sensor nodes to the BC nodes. $\boldsymbol{\Phi}_m\in\mathbb{C}^{N(M-1)\times N(M-1)}=\mathrm{diag}(\beta_1 e^{j\theta_1},\cdots,\beta_k e^{j\theta_k},\cdots,\beta_{N(M-1)}e^{j\theta_{N(M-1)}})$ denotes the backscattering coefficient diagonal matrix of the BC nodes, where $0\leqslant\beta_k\leqslant 1$ and $0\leqslant\theta_k\leqslant 2\pi$ denote the backscattering amplitude and phase shift, respectively. We set $\beta=1$ in this paper for simplicity in derivation. $z'\sim\mathcal{CN}(0,\sigma^2)$ denotes the AWGN at the receiving antenna of the UAV. Thus, the received SNR at the UAV from type m sensor nodes can be expressed as:

$$\begin{aligned}\gamma_m&=\frac{\left|\left(\boldsymbol{g}_{d_m}^T+\boldsymbol{g}_{r_m}^T\boldsymbol{\Phi}_m\boldsymbol{H}_m\right)\boldsymbol{x}_m\right|^2}{\sigma^2}\\&=\frac{\left|\left(\boldsymbol{g}_{d_m}^T\boldsymbol{\Lambda}_m+\boldsymbol{g}_{r_m}^T\boldsymbol{\Phi}_m\boldsymbol{H}_m\boldsymbol{\Lambda}_m\right)\boldsymbol{\omega}_m'\right|^2}{\sigma^2}\frac{\tau_0}{\tau_m},\end{aligned} \quad (6)$$

where

$$\begin{aligned}\boldsymbol{\Lambda}_m&=\mathrm{diag}\left\{\sqrt{P_{m1}^{EH}},\cdots,\sqrt{P_{mn}^{EH}},\cdots,\sqrt{P_{mN}^{EH}}\right\},\\\boldsymbol{\omega}_m'&=\left[e^{j\theta_{m1}^{Tx}},\cdots,e^{j\theta_{mn}^{Tx}},\cdots e^{j\theta_{mN}^{Tx}}\right]^T\in\mathbb{C}^{N\times 1}.\end{aligned} \quad (7)$$

Thus, the throughput of type m sensor nodes can be expressed as:

$$R_m=\tau_m\log_2\left(1+\gamma_m'\frac{\tau_0}{\tau_m}\right), \quad (8)$$

where $\gamma_m'=\frac{\left|\left(\boldsymbol{g}_{d_m}^T\boldsymbol{\Lambda}_m+\boldsymbol{g}_{r_m}^T\boldsymbol{\Phi}_m\boldsymbol{H}_m\boldsymbol{\Lambda}_m\right)\boldsymbol{\omega}_m'\right|^2}{\sigma^2}$.

III. Sum-Throughput Optimization

In this section, the sum-throughput maximization problem of the UAV-assisted WPSN with M sensor types is investigated. $\boldsymbol{\tau}=\left[\tau_0,\tau_1,\cdots,\tau_M\right]^T$, $\boldsymbol{x}=\left[\boldsymbol{x}_1,\cdots,\boldsymbol{x}_M\right]$, and $\boldsymbol{\Phi}=\left[\boldsymbol{\Phi}_1,\cdots,\boldsymbol{\Phi}_M\right]$ are optimizing variables of time allocation, distributed beamforming and BC, respectively. Then, the sum-throughput maximization problem is formulated as follows:

$$\begin{aligned}P1:\ &\max_{\boldsymbol{\tau},\boldsymbol{x},\boldsymbol{\Phi}}\quad\sum_{m=1}^{M}\tau_m\log_2\left(1+\gamma_m'\left(\boldsymbol{x}_m,\boldsymbol{\Phi}_m\right)\frac{\tau_0}{\tau_m}\right),\\&\text{s.t.}\quad\tau_0+\sum_{m=1}^{M}\tau_m=1.\end{aligned} \quad (9)$$

Note that the objective function in problem (9) is a sum of $\tau_m\log_2\left(1+\gamma_m'\left(\boldsymbol{x}_m,\boldsymbol{\Phi}_m\right)\frac{\tau_0}{\tau_m}\right)$ which is a monotonically increasing function over $\gamma_m'\left(\boldsymbol{x}_m,\boldsymbol{\Phi}_m\right)$. $\gamma_m'\left(\boldsymbol{x}_m,\boldsymbol{\Phi}_m\right)$ is a function of $\boldsymbol{x}_m$ and $\boldsymbol{\Phi}_m$, while it is unrelated to $\boldsymbol{\tau}$. Based on this observation, we decompose the above problem into a BC subproblem and a time allocation subproblem, and propose a two-step scheme to solve them. In this way, we can first obtain the optimal values of $\boldsymbol{x}_m$ and $\boldsymbol{\Phi}_m$ by solving a set of subproblems as follows:

$$P1.1:\ \max_{\boldsymbol{x}_m,\boldsymbol{\Phi}_m}\quad\gamma_m'\left(\boldsymbol{x}_m,\boldsymbol{\Phi}_m\right),\ \forall m=1,\cdots,M. \quad (10)$$

After obtaining the optimal value of γ_m' in problem (10) denoted by $\gamma_m'^{*}$, problem (9) can be rewritten as

$$\begin{aligned}P1.2:\ &\max_{\boldsymbol{\tau}}\quad\sum_{m=1}^{M}R_m(\gamma_m'^{*},\tau_0,\tau_m),\\&\text{s.t.}\quad\tau_0+\sum_{m=1}^{M}\tau_m=1.\end{aligned} \quad (11)$$

The optimal value of $\boldsymbol{\tau}$ in problem (9) can be obtained by solving (11). The detailed procedure of the proposed two-step scheme is given in the following two subsections.

A. BC Subproblem

In the first step, we solve subproblem (10) to maximize $\gamma_m', \forall m = 1, \cdots, M$. Subproblem (10) is a joint distributed beamforming and BC optimization problem in information transmission of type m sensor nodes, which is expressed as:

$$\begin{aligned} \max_{\boldsymbol{\theta}_m^{Tx}, \boldsymbol{\theta}_k} \quad & \left| \left(\boldsymbol{g}_{d_m}^T \boldsymbol{\Lambda}_m + \boldsymbol{g}_{r_m}^T \boldsymbol{\Phi}_m \boldsymbol{H}_m \boldsymbol{\Lambda}_m \right) \boldsymbol{\omega}_m' \right| \\ \text{s.t. } & 0 \leq \theta_{mn}^{Tx} \leq 2\pi, \ \forall n = 1, \cdots, N \\ & 0 \leq \theta_k \leq 2\pi, \ \forall k = 1, \cdots, N(M-1), \end{aligned} \tag{12}$$

where the phases of distributed beamforming and BC are denoted by $\boldsymbol{\theta}_m^{Tx} = \left[\theta_{m1}^{Tx}, \cdots, \theta_{mn}^{Tx}, \cdots, \theta_{mN}^{Tx}\right]^T$ and $\boldsymbol{\theta}_k = \left[\theta_1, \cdots, \theta_k, \cdots, \theta_{N(M-1)}\right]$, respectively. The optimal solutions of θ_{mn}^{Tx} can be denoted by $\theta_{mn}^{Tx*} = \arg\left(\omega_{mn}^{MRT}\right)$. ω_m^{MRT} is the maximum-ratio transmission (MRT) beamforming vector which can be expressed as:

$$\boldsymbol{\omega}_m^{MRT} = \frac{\left(\boldsymbol{g}_{d_m}^T \boldsymbol{\Lambda}_m + \boldsymbol{g}_{r_m}^T \boldsymbol{\Phi}_m \boldsymbol{H}_m \boldsymbol{\Lambda}_m \right)^H}{\left\| \boldsymbol{g}_{d_m}^T \boldsymbol{\Lambda}_m + \boldsymbol{g}_{r_m}^T \boldsymbol{\Phi}_m \boldsymbol{H}_m \boldsymbol{\Lambda}_m \right\|}. \tag{13}$$

Substituting θ_{mn}^{Tx*} into (12), we have

$$\begin{aligned} \max_{\boldsymbol{\theta}_k} \quad & \left\| \boldsymbol{g}_{d_m}^T \boldsymbol{\Lambda}_m + \boldsymbol{g}_{r_m}^T \boldsymbol{\Phi}_m \boldsymbol{H}_m \boldsymbol{\Lambda}_m \right\|_1, \\ \text{s.t.} \quad & 0 \leq \theta_k \leq 2\pi, \ \forall k = 1, \cdots, N(M-1). \end{aligned} \tag{14}$$

where $\|\cdot\|_1$ denotes the L_1 norm function. To simplify the expression, we make $\boldsymbol{g}_{r_m}^T \boldsymbol{\Phi}_m \boldsymbol{H}_m \boldsymbol{\Lambda}_m = \boldsymbol{u}_m^T \boldsymbol{\Psi}_m$, where

$$\begin{aligned} & \boldsymbol{\Psi}_m = \operatorname{diag}(\boldsymbol{g}_{r_m}^T) \boldsymbol{H}_m \boldsymbol{\Lambda}_m, \\ & \boldsymbol{u}_m = \left[e^{j\theta_1}, \cdots, e^{j\theta_k}, \cdots, e^{j\theta_{N(M-1)}} \right]^T. \end{aligned} \tag{15}$$

Thus, the objective function in (14) can be rewritten as

$$\begin{aligned} & \left\| \boldsymbol{g}_{d_m}^T \boldsymbol{\Lambda}_m + \boldsymbol{g}_{r_m}^T \boldsymbol{\Phi}_m \boldsymbol{H}_m \boldsymbol{\Lambda}_m \right\|_1 \\ & = \left\| \boldsymbol{g}_{d_m}^T \boldsymbol{\Lambda}_m + \boldsymbol{u}_m^T \boldsymbol{\Psi}_m \right\|_1 \\ & \leqslant \left\| \boldsymbol{g}_{d_m}^T \boldsymbol{\Lambda}_m \right\|_1 + \left\| \boldsymbol{u}_m^T \boldsymbol{\Psi}_m \right\|_1. \end{aligned} \tag{16}$$

Considering the prohibitive computational complexity for a backscatter node to compute the optimal backscattering coefficients,[1] we propose a distributed BC scheme. In the proposed scheme, the backscattering coefficient at a backscatter node is computed only based on the phase of the incident signal at itself and the channel state information (CSI) from the backscatter node to the UAV. The proposed distributed BC scheme is designed to make the phases of received signals at the UAV from direct link and the BC link via backscatter nodes are same, i.e.,

$$\arg(\boldsymbol{g}_{d_m}^T \boldsymbol{\Lambda}_m) = \arg(\boldsymbol{u}_m \boldsymbol{\Psi}_m). \tag{17}$$

Using this distributed BC scheme, each transmitted sensor node only needs the CSI from itself to the UAV for distributed beamforming. The transmitted signal at S_{mn} can be expressed as:

$$x_{mn} = \sqrt{\frac{E_{mn}}{\tau_m T}} e^{j \arg(h_{mn}^H)} s_m, \tag{18}$$

Then, the phases of received signals at the UAV from type m sensor nodes via direct links are same. Meanwhile, the incident signal at a backscatter node k can be represented by

$$s_{in}^{(k)} = \sum_{n=1}^{N} x_{mn} h_{mn,k} \tag{19}$$

where $h_{mn,k} \in \mathbb{C}^{1\times 1}$ denotes the channel from S_{mn} to backscatter node k. To maximize the received signal power at the UAV, backscatter node k adjusts its backscattering coefficient to make the received signals at the UAV via indirect links are same as those in direct links, i.e.,

$$\theta_k^* = \arg(s_{in}^{(k)H} h_{ak}^H) = -\arg(s_{in}^{(k)}) - \arg(h_{ak}). \tag{20}$$

To sum up, a low-complexity distributed beamforming and distributed backscattering scheme is achieved by using $\theta_{mn}^{Tx*} = \arg\left(\omega_{mn}^{MRT}\right)$ at the transmitted sensor nodes and (20) at the BC nodes, respectively.

B. Time Allocation Subproblem

In the second step, we solve subproblem (11) to maximize sum-throughput. Based on the joint distributed beamforming solutions and distributed backscattering solutions which have already been obtained in Section III-A, the sum-throughput maximization problem can be expressed as:

$$\begin{aligned} \max_{\boldsymbol{\tau}} \quad & \sum_{m=1}^{M} \tau_m \log_2(1 + \gamma_m'^* \frac{\tau_0}{\tau_m}), \\ \text{s.t.} \quad & \tau_0 + \sum_{m=1}^{M} \tau_m = 1. \end{aligned} \tag{21}$$

The objective function of problem (21) is the sum of perspective functions of $\log_2(1 + \gamma_m'^* \tau_0)$ which is a concave function. According to the preserve convexity property [18], the objective function of problem (21) is also concave. Thus, problem (21) is a convex optimization problem, and the Lagrange dual function of problem (21) is given as:

$$L = \sum_{m=1}^{M} \tau_m \log_2(1 + \gamma_m'^* \frac{\tau_0}{\tau_m}) - \mu(\tau_0 + \sum_{m=1}^{M} \tau_m - 1), \tag{22}$$

where μ is the Lagrangian multiplier associated with the constraint in (21). According to the Karush-Kuhn-Tucker (KKT) conditions, we have

$$\frac{\partial L}{\partial \tau_0}(\boldsymbol{\tau}^*) = \frac{1}{\ln 2} \sum_{m=1}^{M} \frac{\gamma_m'^*}{1 + x_m} - \mu = 0, \tag{23a}$$

$$\frac{\partial L}{\partial \tau_m}(\boldsymbol{\tau}^*) = \frac{1}{\ln 2} \left(\ln(1 + x_m) - \frac{x_m}{1 + x_m} \right) - \mu = 0, \tag{23b}$$

[1] To obtain the optimal backscattering coefficients, each backscatter node needs a lot of communication resources to obtain the global channel information and a lot of computation resources to compute.

where $x_m = \gamma_m'^* \frac{\tau_0}{\tau_m}$. We define $f(x) = \ln(1+x) - \frac{x}{1+x}$, $x > 0$. By combining (23a) with (23b) and eliminating variable μ, we have

$$f(x_m) = \sum_{i=1}^{M} \frac{\gamma_i'^*}{1+x_i}, \forall i = 1, \cdots, M \tag{24}$$

Since $f(x)$ is monotonically increasing and $f(x_1) = \cdots = f(x_M)$, we have $x_1 = \cdots = x_M = \bar{x}$. Then (24) can be rewritten as

$$\ln(1+\bar{x}) - \frac{\bar{x}}{1+\bar{x}} = \frac{\sum_{i=1}^{M} \gamma_i'^*}{1+\bar{x}}, \tag{25a}$$

$$\Rightarrow \frac{\sum_{i=1}^{M} \gamma_i'^* - 1}{1+\bar{x}} e^{\frac{-1+\sum_{i=1}^{M} \gamma_i'^*}{1+\bar{x}}} = \frac{\left(\sum_{i=1}^{M} \gamma_i'^* - 1\right)}{e} \tag{25b}$$

$$\Rightarrow w(\bar{x}) e^{w(\bar{x})} = \frac{\left(\sum_{i=1}^{M} \gamma_i'^* - 1\right)}{e}, \tag{25c}$$

where $w(\bar{x}) = \frac{\sum_{i=1}^{M} \gamma_i'^* - 1}{1+\bar{x}}$. By using the Lambert W function, the solution of w in (25c) can be obtained and denoted by w^*, then we have $\bar{x} = \frac{\sum_{i=1}^{M} \gamma_i'^* - 1}{w^*} - 1$. According to this expression and $\bar{x} = \gamma_m'^* \frac{\tau_0}{\tau_m}$, we have

$$\tau_m = \frac{\gamma_m'^* w^*}{\sum_{i=1}^{M} \gamma_i'^* - 1 - w^*} \tau_0. \tag{26}$$

According to (26) and the constraint in (9), we can get the closed-form expressions of optimal time allocation solutions as follows:

$$\begin{cases} \tau_0^* = 1 \Big/ \left(1 + \dfrac{w^* \sum_{i=1}^{M} \gamma_i'^*}{\sum_{i=1}^{M} \gamma_i'^* - w^* - 1}\right), \\ \tau_m^* = \dfrac{\gamma_m'^* w^*}{\sum_{i=1}^{M} \gamma_i'^* - w^* - 1} \tau_0, \quad m = 1, 2, \cdots, M. \end{cases} \tag{27}$$

IV. Simulation Results

In this section, extensive simulation results in a UAV-assisted WPSN with various sensor types are provided. Based on the obtained optimal distributed backscattering (ODB) coefficients, we compare the sum-throughput performance of the proposed joint distributed beamforming and BC scheme with the following benchmark schemes:

- **Fixed-coefficient distributed backscattering (FDB) scheme**: In this scheme, all phases of backscattering coefficients are equal to 0, and the time allocations are optimized based on (27).
- **No distributed backscattering (DB) scheme**: In this scheme, only direct transmission is considered in the UAV-assisted WPSN, and γ_m' in problem (9) is equal to $\left|\boldsymbol{g}_{d_m}^T \boldsymbol{\Lambda}_m\right|^2 / \sigma^2$. In addition, the time allocations are optimized based on (27).
- **No DB and equal time allocation (ETA) scheme**: In this scheme, only direct transmission is considered, and the time for WIT is equally allocated.

The spectrum density of AWGN at the receiving antenna is assumed to be -160 dBm/Hz, and the bandwidth is 1 MHz [2]. The average signal power attenuation is assumed to be 30 dB at the reference distance of 1 m. We assume that sensor nodes

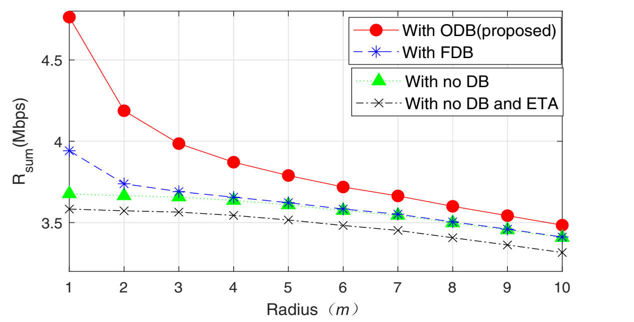

Fig. 4. The average sum-throughput performance versus the coverage radius under different schemes.

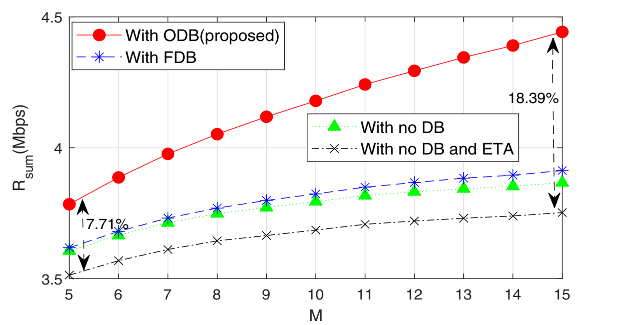

Fig. 5. The average sum-throughput performance versus the number of sensor types under different schemes.

are distributed in a circle with radius R^{loc}, and the locations of sensor nodes are uniformly distributed. In addition, the UAV is placed above the circle center with height D_H. In the non-linear EH model, it is assumed that $a_{mn} = 150$, $b_{mn} = 0.014, \forall m, n$, and $M^{EH} = 24$ mW [17]. Simulation results are averaged based on 2,000 samples with different channel fading and sensor nodes' locations.

Figure 4 shows the impact of the coverage radius on the average sum-throughput performance in the UAV-assisted WPSN with $M = 5$, $N = 5$, $P_a = 1$ W, $D_H = 20$ m, and $\alpha = 2.5$. It is observed that the proposed scheme outperforms the other three schemes especially with small coverage radius. Also, it can be observed that the advantage of two schemes with DB (the proposed scheme and the FDB scheme) is extremely obvious in the situation of small radius.

Next, by fixing $R^{loc} = 5$ m, Fig. 5 shows the average sum-throughput comparison for different numbers of sensor types. With the increasing number of sensor types, there are more sensor nodes acting as backscatter nodes. Then the superiorities of schemes with BC (the proposed scheme and the FDB scheme) are increasingly obvious. When the number of sensor types increases to 15, it is observed that a 18.39% sum-throughput gain is achieved by the proposed scheme as compared to the scheme with no DB and ETA.

Figure 6 reveals the average sum-throughput performance versus the number of sensor nodes in each sensor type, where $M = 5$, $R^{loc} = 5$ m, $P_a = 1$ W, $D_H = 20$ m, and $\alpha = 2.5$. With the increase of the number of sensor nodes in each sensor type, both the number of sensor nodes for distributed

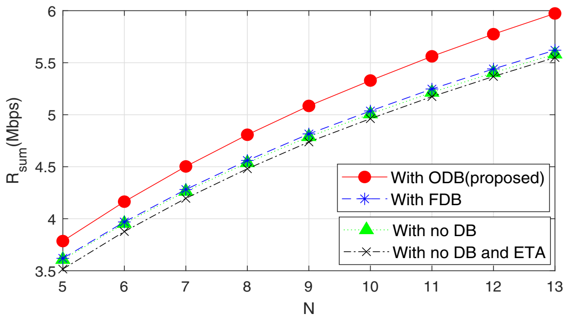

Fig. 6. The average sum-throughput performance versus the sensor number N of each type under different schemes.

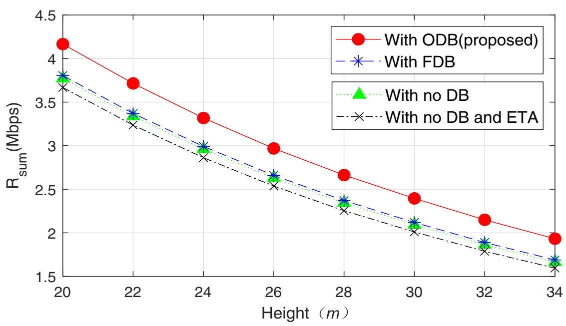

Fig. 7. The average sum-throughput performance versus the UAV height under different schemes.

backscattering and the number of sensor nodes for distributed beamforming increase. Thus, the sum-throughput performance of all four schemes are enhanced dramatically.

As shown in Fig. 7, we further study the average sum-throughput performance over UAV height D_H for different transmission schemes, where $M = 8$, $N = 5$, $R^{loc} = 5\,\text{m}$, $P_a = 1\,\text{W}$ and $\alpha = 2.5$. It is observed that the sum-throughput of all schemes drops with the increase of UAV height because of a high pathloss. The proposed scheme still outperforms other three schemes.

V. Conclusion

In this paper, we have investigated a UAV-assisted WPSN with various types of sensor nodes. A joint distributed beamforming and backscatter cooperation scheme has been proposed to enhance the sum-throughput performance by reducing the impact of long-distance transmission from sensor nodes to the UAV. The proposed scheme can also improve the coverage area and energy efficiency of the UAV. Simulation results have been provided to demonstrate the superiority of the proposed scheme as compared to benchmarks, especially in the scenario with a large number of sensor nodes. For the future work, we will investigate a cooperative transmission scheme considering sensitivity thresholds which can effectively harvest the energy and successfully receive the information.

Acknowledgement

This work was supported by Jilin Provincial Science and Technology Department Key Scientific and Technological Project (No. 20190302031GX, No. 2018020163YY), Changchun Scientific and Technological Innovation Double Ten Project (No. 18SS010), National Natural Science Foundation of China (No. 61671219), and Jilin Province Development and Reform Commission Project (No. 2017C046-3). This work was supported in part by the Natural Sciences and Engineering Research Council (NSERC) of Canada.

References

[1] Y. Zeng and R. Zhang, "Energy-efficient UAV communication with trajectory optimization," *IEEE Trans. Wireless Commun.*, vol. 16, no. 6, pp. 3747–3760, 2017.

[2] H. Ju and R. Zhang, "Throughput maximization in wireless powered communication networks," *IEEE Trans. Wireless Commun.*, vol. 13, no. 1, pp. 418–428, 2014.

[3] R. Zhang, M. Wang, L. X. Cai, and X. Shen, "Learning to be proactive: Self-regulation of UAV based networks with UAV and user dynamics," *IEEE Trans. Wireless Commun.*, 2021. doi:10.1109/TWC.2021.3058533.

[4] X. Shen, J. Gao, W. Wu, K. Lyu, M. Li, W. Zhuang, X. Li, and J. Rao, "AI-assisted network-slicing based next-generation wireless networks," *IEEE Open J. Veh. Technol.*, vol. 1, no. 1, pp. 45–66, 2020.

[5] T. Shen and H. Ochiai, "A UAV-enabled wireless powered sensor network based on NOMA and cooperative relaying with altitude optimization," *IEEE Open J. Commun. Soc.*, vol. 2, pp. 21–34, 2021.

[6] W. Wu, N. Chen, C. Zhou, M. Li, X. Shen, W. Zhuang, and X. Li, "Dynamic RAN slicing for service-oriented vehicular networks via constrained learning," *IEEE J. Sel. Areas Commun.*, vol. 39, no. 7, pp. 2076–2089, Jul. 2021.

[7] S. Suman, S. Kumar, and S. De, "UAV-assisted RFET: A novel framework for sustainable WSN," *IEEE Trans. Green Commun. Netw.*, vol. 3, no. 4, pp. 1117–1131, 2019.

[8] X. Li, C. You, S. Andreev, Y. Gong, and K. Huang, "Wirelessly powered crowd sensing: Joint power transfer, sensing, compression, and transmission," *IEEE J. Sel. Areas Commun.*, vol. 37, no. 2, pp. 391–406, 2019.

[9] W. Wu, N. Cheng, N. Zhang, P. Yang, W. Zhuang, and X. Shen, "Fast mmwave beam alignment via correlated bandit learning," *IEEE Trans. Wireless Commun.*, vol. 18, no. 12, pp. 5894–5908, Dec. 2019.

[10] S. Jayaprakasam, S. K. A. Rahim, and C. Y. Leow, "Distributed and collaborative beamforming in wireless sensor networks: Classifications, trends, and research directions," *IEEE Commun. Surveys Tuts.*, vol. 19, no. 4, pp. 2092–2116, 2017.

[11] S. Gong, X. Huang, J. Xu, W. Liu, P. Wang, and D. Niyato, "Backscatter relay communications powered by wireless energy beamforming," *IEEE Trans. Commun.*, vol. 66, no. 7, pp. 3187–3200, 2018.

[12] W. Chen, H. Ding, S. Wang, D. B. da Costa, F. Gong, and P. H. J. Nardelli, "Backscatter cooperation in NOMA communications systems," *IEEE Trans. Wireless Commun.*, 2021. doi: 10.1109/TWC.2021.3050600.

[13] R. Mudumbai, D. R. Brown Iii, U. Madhow, and H. V. Poor, "Distributed transmit beamforming: Challenges and recent progress," *IEEE Communications Magazine*, vol. 47, no. 2, pp. 102–110, 2009.

[14] J. Xu, Z. Zhong, and B. Ai, "Wireless powered sensor networks: Collaborative energy beamforming considering sensing and circuit power consumption," *IEEE Wireless Commun. Lett.*, vol. 5, no. 4, pp. 344–347, 2016.

[15] H. Ochiai, P. Mitran, H. V. Poor, and V. Tarokh, "Collaborative beamforming for distributed wireless ad hoc sensor networks," *IEEE Trans. Signal Process.*, vol. 53, no. 11, pp. 4110–4124, 2005.

[16] Q. Li, N. Zhang, M. Cheffena, and X. Shen, "Channel-based optimal back-off delay control in delay-constrained industrial WSNs," *IEEE Trans. Wireless Commun.*, vol. 19, no. 1, pp. 696–711, 2019.

[17] E. Boshkovska, D. W. K. Ng, N. Zlatanov, A. Koelpin, and R. Schober, "Robust resource allocation for MIMO wireless powered communication networks based on a non-linear EH model," *IEEE Trans. Commun.*, vol. 65, no. 5, pp. 1984–1999, 2017.

[18] S. Boyd, S. P. Boyd, and L. Vandenberghe, *Convex optimization*. Cambridge university press, 2004.